

DOI: 10.1002/cmdc.200800097

# Phenanthroline Derivatives with Improved Selectivity as DNA-Targeting Anticancer or Antimicrobial Drugs

Sudeshna Roy,<sup>[a]</sup> Katharine D. Hagen,<sup>[a, b]</sup> Palanisamy Uma Maheswari,<sup>[a]</sup> Martin Lutz,<sup>[c]</sup> Anthony L. Spek,<sup>[c]</sup> Jan Reedijk,<sup>\*[a]</sup> and Gilles P. van Wezel<sup>\*[a]</sup>

*Phenanthroline derivatives are of interest due to their potential activity against cancer, and viral, bacterial, and fungal infections. In a search for highly specific antitumor and antibacterial compounds, we report the activities of 1,10-phenanthroline-5,6-dione (phendione or L<sup>1</sup>), dipyrido[3,2-a:2',3'-c]phenazine (dppz or L<sup>2</sup>), and their corresponding platinum complexes ([PtL<sup>1</sup>Cl<sub>2</sub>] and [PtL<sup>2</sup>Cl<sub>2</sub>]), and provide the solid-state 3D structure for [PtL<sup>1</sup>Cl<sub>2</sub>]. It is generally known that a toxic metal ion coordinated to an active organic moiety leads to a synergistic effect; however, we report herein that the platinum complexes [PtL<sup>1</sup>Cl<sub>2</sub>] and [PtL<sup>2</sup>Cl<sub>2</sub>]*

*have weaker activities relative to those of the free ligands, especially against bacteria. Testing these agents against a variety of human cancer cell lines revealed that L<sup>1</sup> and [PtL<sup>1</sup>Cl<sub>2</sub>] were at least as active as cisplatin against several of the cell lines (including a cisplatin-resistant cell line). The absence of antibacterial activity of [PtL<sup>1</sup>Cl<sub>2</sub>] removes the detrimental effect of phenanthrolines toward intestinal flora, suggesting a highly promising new strategy for the development of anticancer drugs with reduced side effects.*

## Introduction

The successful application of cisplatin in cancer chemotherapy and its associated side effects and resistance (intrinsic or acquired), continue to fuel research in platinum chemistry in an effort to formulate new, specific metallodrugs with fewer or no side effects.<sup>[1]</sup> Among several platinum-containing candidates, cisplatin, carboplatin, and oxaliplatin have been approved for clinical use.<sup>[2]</sup> Investigation into the activity of cisplatin at the biomolecular level indicates that genomic DNA is the primary target, where cisplatin forms an adduct with adjacent purine bases,<sup>[3]</sup> particularly with guanine.<sup>[4–6]</sup> This coordination results in distortion of the DNA helix towards the major groove followed by unwinding of the DNA. Finally, the cells undergo apoptosis due to unsuccessful DNA repair.<sup>[7]</sup>

Phenanthrolines are a class of compounds with an entirely different mode of action,<sup>[8]</sup> of interest for their potential activity against cancer as well as and viral, bacterial, and fungal infections. In contrast to cisplatin, intercalating ligands, such as the phenanthrolines and their metal complex derivatives, interact with DNA by aromatic  $\pi$  stacking between base pairs. This interaction results in lengthening, stiffening, and unwinding of the helix.<sup>[8]</sup> The DNA cleaving ability of phenanthroline has made it a frequently used reagent in DNA footprinting studies.<sup>[9,10]</sup> One phenanthroline derivative, phenanthroline-5,6-dione (phendione), displays significant anticancer activity, both with and without a coordinated metal.<sup>[11,12]</sup>

Some specific phenanthroline-7-ones are already well known for their excellent cytotoxic properties. Delfourne et al. have probed the effect of various substituents on different rings of these tetracyclic aromatic compounds.<sup>[13,14]</sup> Phenanthroline itself shows very high activity towards neoplastic cell lines.<sup>[15,16]</sup> The IC<sub>50</sub> values of phenanthroline in L1210 (cisplatin-sensitive murine leukemia), HepG2 (human hepatocellular carcinoma),

and A498 (human kidney adenocarcinoma) cell lines are reported as 5, 4.5, and 5.5  $\mu\text{M}$  respectively. In leukemia cell lines phenanthroline is less active than cisplatin (IC<sub>50</sub> = 2.08  $\mu\text{M}$ <sup>[17]</sup>), whereas in other cell lines it shows 3.3- and 2.5-fold enhanced activity.

Little is known about the antimicrobial activity of these antitumor compounds. It is clear that a detrimental effect on the intestinal flora in addition to the unavoidable consequences of chemotherapy on healthy (dividing) cells is undesirable for the patient. Hence, it is advantageous to develop antitumor drugs that do not possess antibacterial activity. The purpose of this study was to further analyze the possible use of phenanthroline derivatives as anticancer drugs, as well as to assess their antimicrobial activities. This was achieved by modifying the phenanthroline ligand and subsequent biological evaluation of

[a] S. Roy,<sup>+</sup> K. D. Hagen,<sup>+</sup> Dr. P. U. Maheswari, Prof. J. Reedijk, Dr. G. P. van Wezel  
Leiden Institute of Chemistry, Leiden University  
P.O. Box 9502, 2300 RA Leiden (The Netherlands)  
Fax: (+31) 71-527-4671 (J.R.)  
Fax: (+31) 71-527-4340 (G.P.v.W.)  
E-mail: reedijk@chem.leidenuniv.nl  
g.wezel@chem.leidenuniv.nl

[b] K. D. Hagen<sup>+</sup>  
Department of Chemistry, Occidental College  
Los Angeles, CA 90041 (USA)

[c] Dr. M. Lutz, Prof. A. L. Spek  
Bijvoet Center for Biomolecular Research  
Crystal and Structural Chemistry, Utrecht University  
Padualaan 8, 3584 Utrecht (The Netherlands)

[<sup>+</sup>] These authors contributed equally to this work.

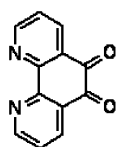
Supporting information for this article is available on the WWW under <http://dx.doi.org/10.1002/cmdc.200800097>.

the derivatives and their platinum complexes using MTT and SRB assays to determine cytotoxicity. Minimum inhibitory concentration (MIC) and zone of inhibition tests were carried out to determine the antimicrobial activities of the derivatives. Because the modifications are to the aromatic ligands, we expect the activity profile to be similar to previous reports.

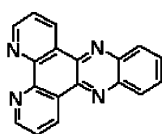
## Results

### Chemical synthesis and structural determination

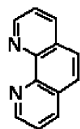
Phenanthroline is a well-known DNA-cleaving agent, which has been used extensively in DNA footprinting studies.<sup>[9,10]</sup> This property also gives rise to significant antitumor activity. Several derivatives of phenanthroline have been described, with varying degrees of activity against eukaryotic cells.<sup>[12,18,19]</sup> To further analyze the possible use of phenanthroline derivatives as anti-cancer drugs, as well as to assess their antimicrobial activities, two derivatives were synthesized: 1,10-phenanthroline-5,6-dione (phendione, L<sup>1</sup>)<sup>[20]</sup> and dipyrido[3,2-*a*:2',3'-*c*]phenazine (dppz, L<sup>2</sup>). These ligands were selected for their subtle differences in aromaticity and coordination properties over the parent ligand (phenanthroline, L<sup>3</sup>).



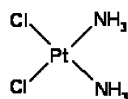
1,10-phenanthroline-5,6-dione (L<sup>1</sup>)



dipyrido[3,2-*a*:2',3'-*c*]phenazine (L<sup>2</sup>)



1,10-phenanthroline (L<sup>3</sup>)



cisplatin

The platinum complexes were produced by coordination of the appropriate ligand (L<sup>1</sup> or L<sup>2</sup>) with a Pt-containing starting material through a spontaneous reaction to give a 1:1 complex. Proton and platinum NMR spectroscopy, and ESI MS were used for structural determination. The structure of [PtL<sup>1</sup>Cl<sub>2</sub>] was determined by X-ray crystallography, and the excellent *R* value obtained confirmed the accuracy in the crystal parameters (Supporting Information, table S1). Carrying out the measurements at low temperature (150 K) significantly improved the data and offers a more accurate description of the structure. Intermolecular and coordinating distances were within the normal range. The crystal structure contains an exceptionally close intermolecular interaction between the S=O group of DMSO and the C5–C6 bond of the metal complex, which may well be the shortest interaction ever reported. A representation of the structure is depicted in Figure 1.

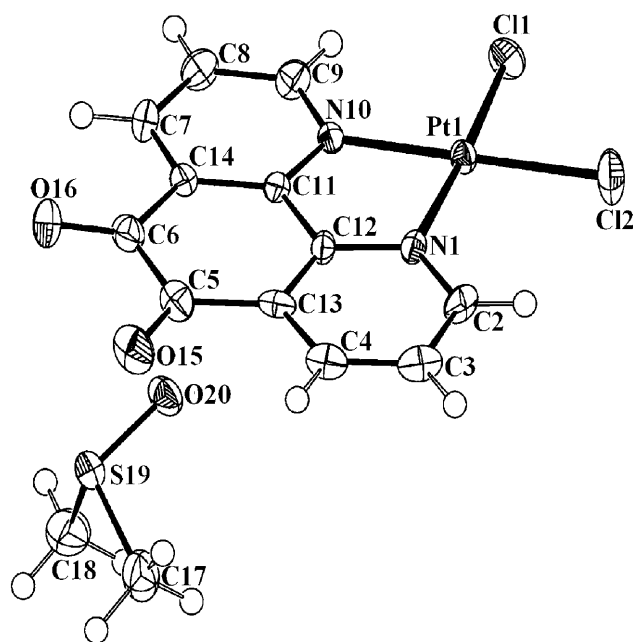


**Figure 1.** 3D molecular structure of [Pt(phendione)Cl<sub>2</sub>](dmsO) as determined by X-ray crystallography (ORTEP diagram with 50% displacement probability).

### In vitro cytotoxicity

The IC<sub>50</sub> values for L<sup>1</sup> and L<sup>2</sup> and their respective platinum complexes were compared with those of cisplatin (Table 1). The cytotoxicity of L<sup>1</sup> was consistently significantly higher than that of L<sup>2</sup>, except against the colon cancer cell line (WIDR), which was found to be equally sensitive to both compounds (IC<sub>50</sub> ~ 3.5 μM), and to a lesser extent against A2780R, the cisplatin-resistant variant of the ovarian carcinoma cell line A2780 (difference less than 1.5-fold). Coordination of ligand L<sup>1</sup> with platinum led to a significant decrease in cytotoxicity, reducing it from 1.4-fold against A2780R, to almost 7-fold against the lung cancer cell line (H226). Results for the corresponding L<sup>2</sup> platinum complex showed an almost complete loss of cytotoxicity against all of the cell lines tested, reducing its activity by 6.1–14-fold and on average by a full order of magnitude.

### Antibacterial activities

One of the main goals of this study was to analyze the antimicrobial activity of the phenanthroline-derived anticancer drugs. For this, we used three representative bacterial strains, namely Gram-negative *Escherichia coli*, and Gram-positive *Bacillus subtilis* (low G+C DNA content) and *Streptomyces coelicolor* (high G+C DNA content). Two tests were conducted using these bacterial strains: a zone of inhibition test and a MIC assay, the details of which are given in the Experimental Section.

The relative antimicrobial activities of the compounds studied were assessed by the measurement of the zone of clearance around a filter disk impregnated with the active agent at 10 mM (Table 2). Because the zones depend on diffusion, the activity decreases exponentially. Surprisingly, whereas dppz (L<sup>2</sup>)

**Table 1.** In vitro IC<sub>50</sub> values of the ligands and platinum complexes toward several neoplastic cell lines and their relative changes in cytotoxicity.

Cell line	IC <sub>50</sub> [μM] cisplatin	IC <sub>50</sub> [μM]				Relative change in cytotoxicity <sup>[a]</sup>		
		L <sup>1</sup>	L <sup>2</sup>	[PtL <sup>1</sup> Cl <sub>2</sub> ]	[PtL <sup>2</sup> Cl <sub>2</sub> ]	L <sup>2</sup> /L <sup>1</sup>	[PtL <sup>1</sup> Cl <sub>2</sub> ]/L <sup>1</sup>	[PtL <sup>2</sup> Cl <sub>2</sub> ]/L <sup>2</sup>
A498	7.50	1.22	4.01	4.90	33.8	3.3	4.0	8.4
EVSA-T	1.40	0.499	2.53	3.05	16.4	6.2	6.2	6.5
H226	10.9	0.494	3.28	3.27	39.8	6.8	6.8	12
IGROV-1	0.563	0.528	3.09	2.67	43.8	5.5	5.1	14
M19-MEL	1.85	0.356	2.77	0.812	20.5	7.9	2.3	7.4
MCF-7	2.32	0.575	2.81	3.38	21.3	4.9	5.9	7.6
WIDR	3.22	3.47	3.65	19.5	45.9	1.1	5.6	13
A2780	5.22	0.068	2.18	0.827	13.2	12	4.6	6.1
A2780R	8.41	0.933	1.33	0.683	19.3	1.4	1.4	14
RF <sup>[b]</sup>	1.61	13.7	0.61	0.829	1.46	–	–	–
Average relative change:						5.5	4.7	9.9

[a] Change in cytotoxicity between ligands (L<sup>2</sup>/L<sup>1</sup>) and between the complex and ligand ([PtL<sup>1</sup>Cl<sub>2</sub>]/L<sup>1</sup> and [PtL<sup>2</sup>Cl<sub>2</sub>]/L<sup>2</sup>). [b] Resistance factor = IC<sub>50</sub>(A2780R)/IC<sub>50</sub>(A2780).

**Table 2.** Zones of inhibition and MIC values against bacterial strains.<sup>[a]</sup>

Compound	Zone of inhibition [diameter in mm] <sup>[b]</sup>			MIC values <sup>[c]</sup> [μg mL <sup>-1</sup> ]	
	<i>E. coli</i>	<i>B. subtilis</i>	<i>S. coelicolor</i>	<i>E. coli</i>	<i>B. subtilis</i>
cisplatin	6 ± 0.6	0	0	25 ± 1	> 200
phenanthroline	6 ± 0.6	9 ± 0.7	9 ± 0.7	25 ± 1	15 ± 1
L <sup>1</sup> (phendione)	16 ± 1	20 ± 1	42 ± 3	2 ± 0.2	0.5 ± 0.1
[PtL <sup>1</sup> Cl <sub>2</sub> ]	0	2 ± 0.2	10 ± 0.5	> 200	> 200
L <sup>2</sup> (dppz)	0	0	0	> 200	> 200
[PtL <sup>2</sup> Cl <sub>2</sub> ]	0	0	0	> 200	> 200

[a] *S. coelicolor* M145; *E. coli*, *E. coli* JM109; *B. subtilis*, *B. subtilis*. [b] Values reported are an average of at least three independent experiments, zones given in mm outside the filter disk. [c] Values reported are an average of at least six growth curves per sample per strain.

did not produce clearance zones, indicative of very low or no antimicrobial activity, phendione (L<sup>1</sup>) had a very strong inhibitory effect on the growth of all strains, giving zones of 16, 20, and 42 mm against *E. coli*, *B. subtilis*, and *S. coelicolor*, respectively. In comparison with the free ligand, [PtL<sup>1</sup>Cl<sub>2</sub>] produced zones against the Gram-positive bacteria, although to a lesser extent, but not against *E. coli*. The [PtL<sup>2</sup>Cl<sub>2</sub>] complex was not found to display any measurable antimicrobial activity.

MIC values in liquid cultures were determined for *E. coli* and *B. subtilis*. (Table 2). Unfortunately, reproducible results could not be obtained using *S. coelicolor* due to poor culture growth, therefore MIC values could not be determined in liquid culture. Similar to the results observed in the zone of inhibition plate tests, L<sup>1</sup> and [PtL<sup>1</sup>Cl<sub>2</sub>] were more active against the Gram-positive *B. subtilis* than against the Gram-negative *E. coli* (Table 2). Ligand L<sup>1</sup> had MIC values of 2 and 0.5 μg mL<sup>-1</sup> against *E. coli* and *B. subtilis*, respectively. These were the lowest MIC values of all compounds tested, validating the results of the previous assay. Although L<sup>1</sup> was at least 100-fold more active than its platinum complex ([PtL<sup>1</sup>Cl<sub>2</sub>]), the complex [PtL<sup>2</sup>Cl<sub>2</sub>] was twofold more active than its free ligand, L<sup>2</sup>. After 16 h, both L<sup>2</sup> and [PtL<sup>2</sup>Cl<sub>2</sub>] showed some precipitation from solution, potentially reducing their effectiveness. Neither L<sup>2</sup> nor its platinum com-

plex inhibited growth of *E. coli* at ≤ 200 μg mL<sup>-1</sup>. However, both of these complexes inhibited growth of *B. subtilis* at 200 μg mL<sup>-1</sup> when incubated for 10 h, after which growth approached control levels.

### DNA cleavage

As phenanthroline efficiently cleaves DNA, it was hypothesized that the antimicrobial activity of L<sup>1</sup> and L<sup>2</sup> arises through a similar mechanism of action. Therefore, the ability of the phenanthroline derivatives and their Pt complexes to cleave DNA was examined. Figure 2 shows the

relative cleavage abilities of all compound concentrations of 25 and 100 μM. Additionally, various dilutions of these compounds were incubated with supercoiled phage φX174 DNA, and the compound concentration necessary to achieve a 1:1 ratio of open circular (OC or nicked DNA) versus linear DNA was noted for comparison (Table 3). Interestingly, the activity of the compounds toward DNA did not follow the trends observed with their antimicrobial activities. In fact, while L<sup>2</sup> displayed a much lower antimicrobial activity against all bacteria tested (Table 2), a 1:1 OC/linear ratio was achieved at 80 μM L<sup>2</sup>, as compared with 125 μM L<sup>1</sup> (Figure 2 and Table 3). The corresponding platinum complexes were far less active than the free ligands, and while some linear DNA was produced, a 1:1 OC/linear ratio was never achieved at concentrations lower than 200 μM. Thus, both L<sup>1</sup> and L<sup>2</sup> are much more effective in cleaving DNA than their platinum complexes.

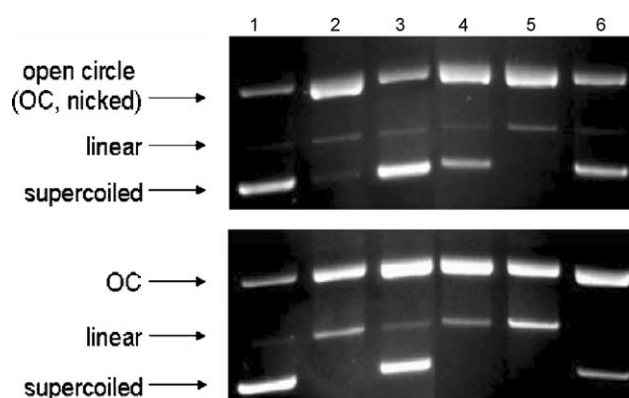


**Figure 2.** Agarose gel electrophoresis showing the effects of phenanthroline-type compounds on DNA integrity. All compounds were incubated at concentrations of 25 μM (top) or 100 μM (bottom), with 20 μM φX174 DNA (in base pairs). Reaction mixtures contained a 4:1:16 ratio of compound/CuSO<sub>4</sub>/ascorbic acid and were incubated for 30 min at 37 °C in the dark. Lane 1: DNA without added compound; lanes 2–6: DNA incubated with L<sup>1</sup> (2), [PtL<sup>1</sup>Cl<sub>2</sub>] (3), L<sup>2</sup> (4), [PtL<sup>2</sup>Cl<sub>2</sub>] (5), CuSO<sub>4</sub> (6.25 μM, top; 25 μM, bottom) and ascorbic acid (100 μM, top; 400 μM, bottom) (6).

Table 3. DNA cleaving activities of ligands and complexes.	
Compound	DNA cleaving activity <sup>[a]</sup> [ $\mu\text{M}$ ]
cisplatin	no linear
phen	15
phendione	125
[PtL <sup>1</sup> Cl <sub>2</sub> ]	> 125
dppz	80
[PtL <sup>2</sup> Cl <sub>2</sub> ]	> 125

[a] The concentration needed to achieve a 1:1 ratio of OC/linear DNA.

### Analysis of DNA conformational changes by circular dichroism

To obtain further insight into the molecular interactions of the ligands L<sup>1</sup> and L<sup>2</sup> and their Pt complex derivatives with DNA,

we performed circular dichroism (CD). Native DNA (calf thymus) gave CD bands at  $\sim 248$  nm (negative) arising due to B-form right-handed helicity, and  $\sim 270$  nm (positive) originating from uniform nucleobase stacking in the B-form conformation.<sup>[21]</sup> When the free ligands L<sup>1</sup> and L<sup>2</sup> and the platinum complexes [PtL<sup>1</sup>Cl<sub>2</sub>] and [PtL<sup>2</sup>Cl<sub>2</sub>] were allowed to interact with DNA, prominent changes were observed in helical conformation, indicative of strong binding of the compounds to DNA. (Figure 3).

The CD spectrum of ligand L<sup>1</sup> differs significantly from that of native DNA, with new bands at 237 (positive) and 252 nm (negative), revealing a complete conformational change in the DNA; the new ellipticity at  $\sim 300$  nm is typical of Z-form DNA.<sup>[22,23]</sup> (Figure 3 a). Moreover, with an increase in incubation time from 6 to 12 h, the negative band at  $\sim 300$  nm increased

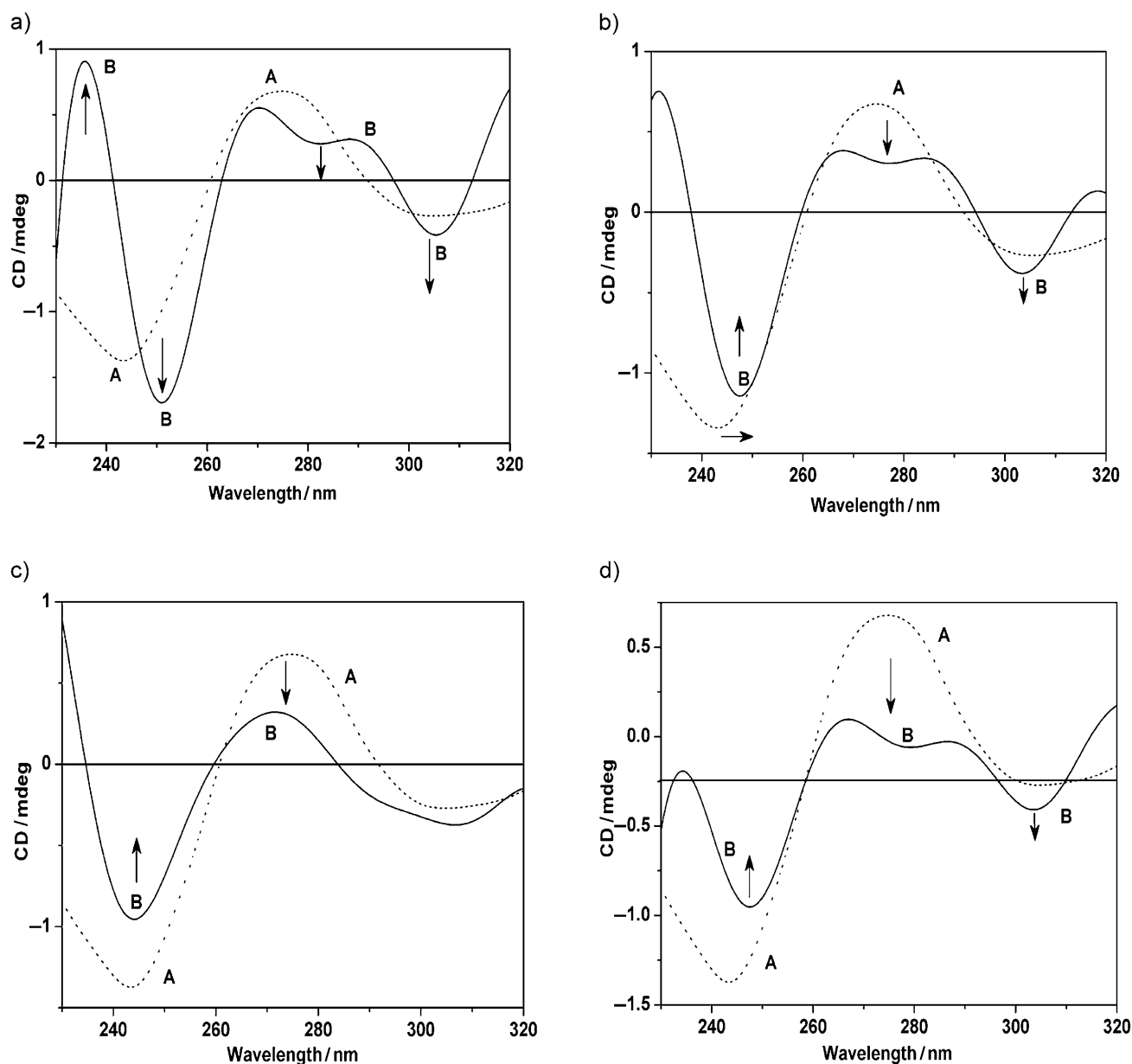


**Figure 3.** Circular dichroism for the analysis of the effect of a) phenidione (L<sup>1</sup>), c) dppz (L<sup>2</sup>), and their Pt complexes b) and d), respectively, on the conformation of calf thymus DNA. Prominent changes in CD spectra were observed in relation to native DNA (trace A) induced by the ligands and their platinum complexes (trace B).

while the positive band at  $\sim 272$  nm decreased. The platinum complex of  $L^1$  produced similar conformational changes in the DNA, although these were less pronounced than for the free ligand (Figure 3b). This is probably due to the coordination of  $[PtL^1Cl_2]$  to the DNA helix leading to control of the conformational change.

The free ligand  $L^2$  shows a decrease in the intensity of both the positive and negative bands, depicting a classical intercalation involving a slight decrease in DNA helicity and base stacking (Figure 3c). The corresponding  $[PtL^2Cl_2]$  complex showed a significantly greater change in the positive band, with the appearance of a new peak at 287 nm (Figure 3d). The appearance of new ellipticity at 237 nm indicates a conformational change in DNA similar to that observed for  $[PtL^1Cl_2]$ . The prominent changes in the CD spectra of the free ligand  $L^2$  and the platinum complex  $[PtL^2Cl_2]$  can be easily explained by different modes of interaction with DNA; the free ligand is only able to intercalate with DNA, whereas the complex is able to both intercalate and coordinate DNA.

## Discussion

The results of this study illustrate the potential application of the phenanthroline derivatives as antimicrobial and antitumor agents. The free ligands, phendione ( $L^1$ ), and dppz ( $L^2$ ), have cytotoxicities similar to those of cisplatin. However, little was known of the antimicrobial activity of phenanthroline derivatives. This study has clearly shown that phendione ( $L^1$ ) is a very potent antibiotic, and importantly, towards both Gram-positive and Gram-negative bacteria. In fact, to our knowledge, there are no reports of a more potent antibiotic against *Streptomyces coelicolor* (unpublished data). In contrast to phendione ( $L^1$ ), dppz ( $L^2$ ) has negligible antimicrobial activity, making it potentially suitable for development as a specific antitumor drug. Indeed,  $L^2$  displays lower  $IC_{50}$  values than cisplatin for four of the nine cell lines, including the cisplatin-resistant cell line A2780R.

It has been well documented that metal complexes bind to DNA through coordination, and this gives rise to the anticancer activity of platinum complexes. Lippard's pioneering work showed that square-planar  $Pt^{II}$  complexes interact non covalently with DNA by intercalation, groove binding, or external electrostatic binding.<sup>[24]</sup> However, the  $Pt^{II}$  complex-DNA adduct is only formed after hydrolysis of one or more of the labile ligands. Because we incorporate both known intercalator ligands and labile chlorido ligands in the complexes synthesized, the combined action is expected. The intercalating property of the ligand increases with extension of the aromatic system, which is evident in the results obtained for our complexes. The complex  $[PtL^2Cl_2]$  has an extended diimine, which gives rise to more prominent changes in the DNA ( $\lambda_{280}$  and  $\lambda_{250}$  positive and negative bands, respectively; Figure 3d) relative to those seen for  $[PtL^1Cl_2]$  (Figure 3b).

The cytotoxic and antimicrobial activities of the compounds may well be explained by their ability to cleave DNA. Surprisingly however, whereas  $L^1$  is both more cytotoxic and has higher antimicrobial activity than  $L^2$ , the latter has a somewhat

higher nuclease activity in vitro. The disparity between the observed activities in vitro and those seen in the cell-based assays strongly suggests that additional factors influence the potency of these compounds, with differences in transport efficiency as one of the most likely explanations. It is unlikely that the cytotoxic activity of the free ligands is due to scavenging of rare metals, as the addition of an excess in trace elements did not affect the antimicrobial activity of  $L^1$  (data not shown). Coordination with platinum significantly altered the activity of the compounds. The in vitro assays showed that the chemical nuclease activity of  $[PtL^1Cl_2]$  was significantly lower than that of phendione ( $L^1$ ) itself, as  $[PtL^1Cl_2]$  produced almost no linear DNA, and supercoiled DNA was still observed even at the higher concentration (100  $\mu$ M). The decreased chemical nuclease activity agrees with the less pronounced changes in DNA conformation observed in the CD studies elicited by  $[PtL^1Cl_2]$  relative to those seen with  $L^1$ , and correlates well to the observed 7-fold decrease in cytotoxicity in coordination with platinum. Similarly, coordinating platinum to  $L^2$  also strongly decreased its activity against eukaryotic cells by up to 14-fold. However, in contrast to  $L^1$ , the chemical nuclease activity of  $L^2$  increased on coordination with platinum. This again underlines the difficulties involved in using in vitro (nuclease) activities to predict the results of cell-based assays. The reduced antimicrobial and cytotoxic activities of dppz ( $L^2$ ) and  $[PtL^2Cl_2]$  in comparison with the analogous phendione compounds ( $L^1$  and  $[PtL^1Cl_2]$ ) may be explained by the limited solubility of  $L^2$  and  $[PtL^2Cl_2]$  in buffer solutions. Formulation to increase the solubility of dppz ( $L^2$ ) may make it a more potent antibiotic.

The ability of compounds such as phendione ( $L^1$ ) to act as dual antitumor and antimicrobial drugs raises an important issue. There is little discussion in the literature on the potential antibacterial activity of (DNA-targeting) drugs, even though some, like phendione, are very potent antibacterial agents and as such will eradicate the intestinal flora that are necessary for, among other things, resistance to invasive pathogenic bacteria. In light of this, phendione itself is perhaps a less obvious candidate for development as a specific antibacterial or antitumor agent. However, considering its strong activities, it is worthy of further investigation to assess whether modifications to phendione could make it a potent antitumor agent but an ineffective antimicrobial, or vice versa. Coordinating platinum to the free ligand is a particularly promising modification. This compound,  $[PtL^1Cl_2]$ , is similar to or more effective than cisplatin against five of the nine cell lines tested, including the cisplatin-resistant line A2780R, while it has almost negligible antimicrobial activity.

## Conclusions

We have demonstrated that phendione ( $L^1$ ) has very strong antimicrobial activity in addition to its antitumor activity. This is a clear example of the care that should be taken with administering DNA-targeting drugs, such as phendione, as anticancer agents. We were able to enhance the specificity of phendione by coordination to platinum, which resulted in dramatically reduced antibacterial activity whilst maintaining potent antitu-



mor activity. Compared with cisplatin, this Pt complex was over twelvefold more potent toward the cisplatin-resistant cell line A2780R. Further modification of phendione ( $L^1$ ) to dppz ( $L^2$ ), extending the aromaticity and planarity of the ligand, appears to be another very efficient way to decrease its antimicrobial activity. While perhaps less potent against cancer cell lines than phendione ( $L^1$ ), dppz ( $L^2$ ) still shows sixfold greater activity than cisplatin against the resistant cell line, A2780R. These results underscore the exciting prospects for phenanthroline derivatives and their platinum complexes as novel anticancer drugs.

## Experimental Section

The solvents used for synthesis were purchased from Biosolve (AR grade) and used without further purification.  $K_2[PtCl_4]$  was provided by Johnson-Matthey (Reading, UK). Phenanthroline, MTT (3-(4,5-dimethylthiazol-2-yl)-2,5-diphenyltetrazolium bromide), and deuterated solvents were purchased from Sigma-Aldrich. RPMI and fetal calf serum (FCS) were obtained from Life Technologies (Paisley, UK). sulforhodamine B (SRB), DMSO, penicillin, and streptomycin were obtained from Duchefa Biochemie B.V. (Haarlem, The Netherlands). TCA and acetic acid were purchased from Baker B.V. (Deventer, The Netherlands) and the phosphate-buffered saline solution (PBS), from NPBI B.V. (Emmer-Compascuum, The Netherlands).

## Chemistry

$^1H$  and  $^{13}C$  spectra were recorded at 300 MHz using a Bruker spectrometer at 25 °C in  $[D_6]DMSO$ . The  $^{195}Pt$  spectra were recorded on a 300 MHz Bruker spectrometer with a 5 mm multi-nucleus probe at 25 °C in  $[D_6]DMSO$  and  $[D_7]DMF$ , using  $Na_2PtCl_6$  as an external reference ( $\delta = 0$  ppm). ESI MS spectra were recorded on a Finnigan AQA instrument equipped with an electrospray ionization (ESI) interface. The ligands phendione (1,10-phenanthroline-5,6-dione<sup>[20]</sup>) and dppz (dipyrido[3,2-*a*:2',3'-*c*]phenazine<sup>[25]</sup>) were synthesized according to published methods. Cisplatin was synthesized from  $K_2[PtCl_4]$  following a classical synthetic route.<sup>[26]</sup> The *cis*- $[Pt(dmsO)_2Cl_2]$  complex was prepared from  $K_2[PtCl_4]$  as described previously.<sup>[27]</sup>

## Synthesis

**$[Pt(1,10\text{-phenanthroline-5,6-dione})Cl_2]$  ( $[PtL^1Cl_2]$ ):** A solution of 1,10-phenanthroline-5,6-dione (50.64 mg, 0.2409 mmol) in EtOH was added dropwise to a solution of  $K_2[PtCl_4]$  (100 mg, 0.2409 mmol) in  $H_2O$  in the dark and stirred overnight at 50 °C. The reaction mixture was filtered, and the precipitate was washed with ice-cold ethanol ( $3 \times 2$  mL) and diethyl ether ( $3 \times 5$  mL), then dried under vacuum in the dark to yield a deep-green precipitate (65.98 mg, 62%);  $^{195}Pt$  NMR (300 MHz,  $[D_7]DMF$ ):  $\delta = -2313$  ppm,  $[N_2Cl_2Pt]$ ;  $^{195}Pt$  NMR (300 MHz,  $[D_6]DMSO$ ):  $\delta = -2317$  ppm,  $[N_2Cl_2Pt]$ ; MS (ESI)  $m/z = 519$   $[Pt(phendione)Cl(DMSO)]^+$ .

**$[Pt(dipyrido[3,2\text{-}a:2',3'\text{-}c]phenazine)Cl_2]$  ( $[PtL^2Cl_2]$ ):** This complex was synthesized as described previously.<sup>[28]</sup> In brief, a solution of *cis*- $[Pt(dmsO)_2Cl_2]$  in DMSO was treated with dppz (1 equiv) and allowed to react overnight in the dark.  $^{195}Pt$  NMR (300 MHz,  $[D_6]DMSO$ ):  $\delta = -2954$  ppm ( $N_2Cl_2Pt$ ); MS (ESI)  $m/z = 547.8$   $[Pt(dppz)Cl_2]$ , 586.8  $[Pt(dmsO)(dppz)(CH_3OH)]^{2+}$ , 659.7  $[Pt(dmsO)_2(dppz)]^{2+}$ .

## Structural determination of $[PtL^1Cl_2]$ by X-ray diffraction

Single crystals were obtained from a solution of  $[PtL^1Cl_2]$  in  $[D_6]DMSO$  at room temperature in the dark. X-ray reflections were measured on a Nonius Kappa CCD diffractometer with rotating anode (graphite monochromator,  $\lambda = 0.71073$  Å). Data were integrated with EvalCCD<sup>[29]</sup> using an accurate description of the experimental setup for the prediction of the reflection contours. Absorption correction and scaling were performed using SADABS.<sup>[30]</sup> The structure was solved with automated Patterson methods (DIRDIF-99<sup>[31]</sup>) in the triclinic space group  $P\bar{1}$  (no. 1). The structure was then transformed to the correct space group  $Cc$  (no. 9) using the ADDSYM routine in PLATON.<sup>[32]</sup> Refinement was performed with SHELXL-97<sup>[33]</sup> against the  $F^2$  of all reflections. Non-hydrogen atoms were refined with anisotropic displacement parameters. All hydrogen atoms were introduced in calculated positions and refined with a riding model. Geometry calculations and higher symmetry checks were performed using PLATON.<sup>[32]</sup> This structure has been previously determined at room temperature and with less accuracy, however, its coordinates (PESZUJ) have not been reported in the Cambridge Structural Database (CSD).<sup>[34]</sup> Additionally, a preliminary X-ray structure was published, in a different space group and packing, but with the same molecular structure.<sup>[35]</sup> The structure described herein is presently the most accurate available, and all relevant structural data have been submitted to the Cambridge Crystallographic Data Centre (CCDC) and are available in the CSD (CCDC 678530). These data can be obtained free of charge from the Cambridge Crystallographic Data Centre via [http://www.ccdc.cam.ac.uk/data\\_request/cif](http://www.ccdc.cam.ac.uk/data_request/cif). Further details of the molecular structure are given in the Supporting Information (tables S1 and S2).

## Biology

Cell culture and microwell plates were obtained from NUCLON (Roskilde, Denmark). The human ovarian carcinoma cell lines A2780 (cisplatin-sensitive) and A2780R (cisplatin-resistant) were donated by Dr. J. M. Pérez (Universidad Autonoma de Madrid, Spain). The cells were grown as monolayers in Dulbecco's modified Eagle's medium (DMEM) supplemented with 10% FCS, penicillin ( $100 U mL^{-1}$ ) and streptomycin ( $100 \mu g mL^{-1}$ ) or in RPMI 1640 medium (ATCC catalog no. 30-2001). The cell lines and bacterial strains used in this study are summarized in Table 4.

## MTT cytotoxicity assay

In-house cytotoxicity tests were performed using the MTT colorimetric method<sup>[36]</sup> adapted as before from our laboratory.<sup>[37,38]</sup> For this, cells were plated onto 96-well sterile plates in  $100 \mu L$  DMEM/FCS medium at a density of  $\sim 2 \times 10^3$  cells per well and incubated for 48 h at 37 °C in 7%  $CO_2$ . Stock solutions were made in DMSO (5 mg in 1 mL solvent) and diluted with medium in such a way that the final concentration of DMSO was consistently less than 1%. Each compound was tested at six final concentrations ranging from 0.4 to 90  $\mu M$ . Cisplatin was tested both in DMSO and in aqueous solution to allow comparison with reported  $IC_{50}$  values. For the assays, after incubation for 48 h, freshly prepared MTT (5  $mg mL^{-1}$  in PBS) was added to each well ( $50 \mu L well^{-1}$ ), and the plates were incubated for a further 3 h at 37 °C. The absorbance at 595 nm was assessed for each well using a Tecan Genios microplate reader. All tests were repeated in triplicate with four biological replicates per experiment for each cell line. The  $IC_{50}$  values were calculated from

**Table 4.** Cell lines and bacterial strains used in this study.

Cell line	Cancer type	Comment <sup>[a]</sup>	Reference
MCF-7	breast cancer	ER + /PgR +	[43]
EVSA-T	breast cancer	ER – /PgR –	[43]
WIDR	colon cancer	–	[43]
IGROV-1	ovarian cancer	–	[43]
M19-MEL	melanoma	–	[43]
A498	renal cancer	–	[43]
H226	non-small-cell lung cancer	–	[43]
MCF-7	breast cancer	cisplatin sensitive	[43]
A2780	human ovarian carcinoma	cisplatin sensitive	[44]
A2780R	human ovarian carcinoma	cisplatin resistant	[44]
Bacterium		Comment	Reference
<i>Escherichia coli</i> JM109		Gram-negative	[45]
<i>Bacillus subtilis</i> 168		Low GC Gram-positive	ATCC culture collection
<i>Streptomyces coelicolor</i> M145		High GC Gram-positive	[40]

[a] ER: estrogen receptor; PgR: progesterone receptor.

the curves drawn by plotting cell survival (%) versus complex concentration ( $\mu\text{M}$ ) using GraphPad Prism v.3.0.

### SRB cytotoxicity test

The microculture SRB test<sup>[39]</sup> was carried out commercially at Pharmachemie (Haarlem, The Netherlands). The human tumor cell lines used were WIDR, IGROV-1, M19-MEL, A498, H226, MCF-7 (ER+, PgR+), and EVSA-T (ER–, PgR–) (Table 4). All cell lines were maintained in continuous logarithmic culture in RPMI 1640 medium with Hepes and phenol red. The medium was supplemented with 10% FCS, penicillin ( $100 \text{ U mL}^{-1}$ ), and streptomycin ( $100 \mu\text{g mL}^{-1}$ ). The cells were treated with trypsin for passage and for use in the assay. Trypsin-treated tumor cells ( $150 \mu\text{L}$ ,  $\sim 2 \times 10^3$  cells  $\text{well}^{-1}$ ) were pre-incubated for 48 h at  $37^\circ\text{C}$  in 96-well, flat-bottom cell culture plates, and the compounds were added in a threefold dilution series up to and including  $62.5 \mu\text{g mL}^{-1}$ . After seven days, cells were fixed with 10% TCA in PBS and incubated at  $4^\circ\text{C}$  for 1 h. The cells were washed with water ( $3 \times$ ) and then stained for 15 min with 0.4% SRB in 1% acetic acid. Subsequently, the cells were washed with 1% acetic acid, air dried, and the bound stain dissolved in unbuffered Tris base ( $150 \mu\text{L}$ ,  $10 \text{ mM}$ ).  $A_{540}$  values were measured using an automated microplate reader (Labsystems Multiskan MS). The concentration–response curves and  $\text{ID}_{50}$  values were calculated using Deltasoft 3 software (Biometallics Inc., Princeton, NJ, USA) and subsequent unit conversion provided the  $\text{IC}_{50}$  values for all samples tested.

### Circular dichroism

The circular dichroic spectra were recorded using a JASCO J-815 spectropolarimeter equipped with a Peltier temperature control unit. All experiments were performed using a quartz cuvette with a path length of 1 mm. Spectra were recorded at standard sensitivity (100 mdeg), with a data pitch of 0.5 nm in the continuous mode. All the spectra were averaged after four accumulations with a scanning speed of  $100 \text{ nm min}^{-1}$  and a response time of 1 s. The baseline was corrected using a reference of 10 mM PBS. The compound ( $1 \times 10^{-3} \text{ M}$ ) together with calf thymus DNA ( $1 \times 10^{-4} \text{ M}$ ) were incubated at  $37^\circ\text{C}$ , and spectra were recorded at the given time intervals. Cisplatin was also tested as a reference compound for comparison.

### Zone of inhibition plate tests

The zone of inhibition tests were carried out on minimal medium agar plates (MM)<sup>[40]</sup> using 1% glucose (*S. coelicolor*) or Luria–Bertani (LB) agar plates (*E. coli* and *B. subtilis*). Approximately  $10^7$  cells (*E. coli* and *B. subtilis*) or spores (*S. coelicolor*) were mixed with soft agar ( $\sim 3 \text{ mL}$  per  $20 \text{ cm}^2$  LB containing 0.7% agar) and plated. Sterile Whatman filters (6 mm) were then placed onto the bacteria-containing top agar layer, and a solution of the compound to be tested ( $10 \mu\text{L}$  containing 100 nM) was spotted onto the filter. The plates were first incubated for 2 h at  $4^\circ\text{C}$  to allow the compounds to diffuse into the agar, then subsequently incubated for 48 h at  $30^\circ\text{C}$  (*S. coelicolor*) and 16 h at  $37^\circ\text{C}$  (*E. coli* and *B. subtilis*). Zone diameters are expressed as the distance to the outer edge of the filter disk (e.g., a zone of 16 mm is noted as 10 mm). Values reported are an average of at least three independent experiments.

### Minimum inhibitory concentration in liquid-grown cultures

*E. coli* (JM109) and *B. subtilis* were inoculated in  $200 \mu\text{L}$  LC cultures with final compound concentrations of  $10 \text{ ng mL}^{-1}$  to  $200 \mu\text{g mL}^{-1}$ , and grown at  $37^\circ\text{C}$  for 16 h with continuous, intensive shaking using a Bioscreen C microbiology shaker/reader (Transgalactic Ltd.), which allows the high-throughput generation of multiple highly reproducible growth curves.<sup>[41,42]</sup> The turbidity was measured at 10-minute intervals using a 450–600 nm wideband filter. All assays were carried out at 10 different dilutions per compound tested and repeated in triplicate. MIC values are defined as the lowest concentration of compound at which growth is completely inhibited for at least 8 h.

### DNA cleaving activity assays

Supercoiled  $\phi\text{X174}$  phage DNA was incubated with various concentrations of the relevant compounds in 10 mM phosphate buffer (pH 7). All assays contained  $\phi\text{X174}$  (20  $\mu\text{M}$  base pairs final concentration) and a 4:1:16 ratio of compound/ $\text{CuSO}_4$ /ascorbic acid, unless otherwise noted. This mixture, with the absence of a compound, was used as the control, as ascorbic acid and  $\text{CuSO}_4$  themselves elicit an unfolding effect on DNA. Samples were incubated in the dark at  $37^\circ\text{C}$  for 30 min. After incubation, reactions were quenched by the addition of DNA loading buffer containing the copper(I) chelator bathocuproine disulfonic acid (BCDA) 1 mM. Samples were run on a 1% agarose gel in TAE buffer, stained with ethidium bromide, and imaged with a BioRad ChemiDoc XRS apparatus.

### Acknowledgements

We are grateful to Prof. Dr. Jaap Brouwer and Hans den Dulk for their excellent experimental support (in-house cytotoxicity), to Pharmachemie, PCN, Haarlem (The Netherlands) for conducting

the cytotoxicity tests and to Dr. Sharief Barends for discussions. K.H. was a US–Netherlands scientific exchange student supported in part by a Howard Hughes Medical Institute Undergraduate Science Education Grant, a grant from the Paul K. and Evalyn E. Richter Trusts Academic Student Project Program, and by grants from the Netherlands Organization for Scientific Research (NWO) to J.R. (grant # 700.53.310) and G.P.v.W. (grant # 700.54.002). Johnson-Matthey (Reading, UK) are gratefully thanked for their generous donation of  $K_2[PtCl_4]$ .

**Keywords:** antibiotics · cancer · chemotherapy · cytotoxicity · phenanthrolines

- [1] E. Wong, C. M. Giandomenico, *Chem. Rev.* **1999**, *99*, 2451–2466.
- [2] D. Wang, S. J. Lippard, *Nat. Rev. Drug Discovery* **2005**, *4*, 307–320.
- [3] A. M. J. Fichtinger-Schepman, J. L. van der Veer, J. H. J. den Hartog, P. H. M. Lohman, J. Reedijk, *Biochemistry* **1985**, *24*, 707–713.
- [4] J. Reedijk, *Proc. Natl. Acad. Sci. USA* **2003**, *100*, 3611–3616.
- [5] J. Reedijk, *Chem. Rev.* **1999**, *99*, 2499–2510.
- [6] J. Reedijk, *Chem. Commun.* **1996**, 801–806.
- [7] D. B. Zamble, T. Jacks, S. J. Lippard, *Proc. Natl. Acad. Sci. USA* **1998**, *95*, 6163–6168.
- [8] S. Kemp, N. J. Wheate, S. Wang, J. G. Collins, S. F. Ralph, A. I. Day, V. J. Higgins, J. R. Aldrich-Wright, *J. Biol. Inorg. Chem.* **2007**, *12*, 969–979.
- [9] A. G. Papavassiliou, *Biochem. J.* **1995**, *305*, 345–357.
- [10] A. G. Papavassiliou, *Methods Mol. Biol.* **1994**, *30*, 43–78.
- [11] M. Devereux, O. S. D. A. Kellett, M. McCann, M. Walsh, D. Egan, C. Deegan, K. Kedziora, G. Rosair, H. Muller-Bunz, *J. Inorg. Biochem.* **2007**, *101*, 881–892.
- [12] C. Deegan, B. Coyle, M. McCann, M. Devereux, D. A. Egan, *Chem.-Biol. Interact.* **2006**, *164*, 115–125.
- [13] E. Delfourne, R. Kiss, L. Le Corre, F. Dujols, J. Bastide, F. Collignon, B. Lesur, A. Frydman, F. Darro, *J. Med. Chem.* **2003**, *46*, 3536–3545.
- [14] E. Delfourne, R. Kiss, L. Le Corre, F. Dujols, J. Bastide, F. Collignon, B. Lesur, A. Frydman, F. Darro, *Bioorg. Med. Chem.* **2004**, *12*, 3987–3994.
- [15] B. Thati, A. Noble, B. S. Creaven, M. Walsh, K. Kavanagh, D. A. Egan, *Eur. J. Pharmacol.* **2007**, *569*, 16–28.
- [16] W. D. McFadyen, L. P. G. Wakelin, I. A. G. Roos, V. A. Leopold, *J. Med. Chem.* **1985**, *28*, 1113–1116.
- [17] A. Garza-Ortiz, H. den Dulk, J. Brouwer, H. Kooijman, A. L. Spek, J. Reedijk, *J. Inorg. Biochem.* **2007**, *101*, 1922–1930.
- [18] N. J. Wheate, R. I. Taleb, A. M. Krause-Heuer, R. L. Cook, S. Wang, V. J. Higgins, J. R. Aldrich-Wright, *Dalton Trans.* **2007**, 5055–5064.
- [19] M. McCann, B. Coyle, S. McKay, P. McCormack, K. Kavanagh, M. Devereux, V. McKee, P. Kinsella, R. O'Connor, M. Clynes, *Biomaterials* **2004**, *17*, 635–645.
- [20] M. Yamada, Y. Tanaka, Y. Yoshimoto, S. Kuroda, I. Shimao, *Bull. Chem. Soc. Jpn.* **1992**, *65*, 1006–1011.
- [21] V. I. Ivanov, L. E. Minchenko, A. K. Schyolki, A. I. Poletaye, *Biopolymers* **1973**, *12*, 89–110.
- [22] J. H. Riazance, W. A. Baase, W. C. Johnson, K. Hall, P. Cruz, I. Tinoco, *Nucleic Acids Res.* **1985**, *13*, 4983–4989.
- [23] S. M. Mirkin, *Front. Biosci.* **2008**, *13*, 1064–1071.
- [24] S. J. Lippard, *Nat. Chem. Biol.* **2006**, *2*, 504–507.
- [25] J. E. Dickeson, L. A. Summers, *Aust. J. Chem.* **1970**, *23*, 1023–1027.
- [26] S. C. Dhara, *Indian J. Chem.* **1970**, *8*, 193–196.
- [27] J. Price, R. Schramm, B. Wayland, A. Williams, *Inorg. Chem.* **1972**, *11*, 1280–1284.
- [28] A. Klein, T. Scheiring, W. Kaim, *Z. Anorg. Allg. Chem.* **1999**, *625*, 1177–1180.
- [29] A. J. M. Duisenberg, L. M. J. Kroon-Batenburg, A. M. M. Schreurs, *J. Appl. Crystallogr.* **2003**, *36*, 220–229.
- [30] SADABS: Siemens Area Detector Absorption Correction Program, G. M. Sheldrick, Universität Göttingen, Göttingen, Germany, **1999**.
- [31] P. T. Beurskens, G. Admiraal, G. Beurskens, W. P. Bosman, S. Garcia-Granda, R. O. Gould, J. M. M. Smits, C. Smykalla, University of Nijmegen, Nijmegen, The Netherlands, **1999**.
- [32] A. L. Spek, *J. Appl. Crystallogr.* **2003**, *36*, 7–13.
- [33] G. M. Sheldrick, *Acta Crystallogr. Sect. A* **2007**, *64*, 112–122.
- [34] R. M. Granger II, R. Davies, K. A. Wilson, E. Kennedy, B. Vogler, Y. Nguyen, E. Mowles, R. Blackwood, A. Ciric, P. S. White, *J. Undergrad. Chem. Res.* **2005**, *2*, 47–50.
- [35] R. Okamura, T. Fujihara, T. Wada, K. Tanaka, *Bull. Chem. Soc. Jpn.* **2006**, *79*, 106–112.
- [36] T. Mosmann, *J. Immunol. Methods* **1983**, *65*, 55–63.
- [37] E. Pantoja, A. Gallipoli, S. van Zutphen, S. Komeda, D. Reddy, D. Jaganyi, M. Lutz, D. M. Tooke, A. L. Spek, C. Navarro-Ranninger, J. Reedijk, *J. Inorg. Biochem.* **2006**, *100*, 1955–1964.
- [38] S. van Zutphen, M. S. Robillard, G. A. van der Marel, H. S. Overkleeft, H. den Dulk, J. Brouwer, J. Reedijk, *Chem. Commun.* **2003**, 634–635.
- [39] Y. P. Keepers, P. E. Pizao, G. J. Peters, J. van Ark-Otte, B. Winograd, H. M. Pinedo, *Eur. J. Cancer* **1991**, *27*, 897–900.
- [40] T. Kieser, M. J. Bibb, M. J. Buttner, K. F. Chater, D. A. Hopwood, *Practical Streptomyces genetics*, The John Innes Foundation, Norwich, UK, **2000**.
- [41] E. Lowdin, I. Odenholt, O. Cars, *Antimicrob. Agents Chemother.* **1998**, *42*, 2739–2744.
- [42] J. Allen, H. M. Davey, D. Broadhurst, J. J. Rowland, S. G. Oliver, D. B. Kell, *Appl. Environ. Microbiol.* **2004**, *70*, 6157–6165.
- [43] M. R. Boyd, *Status of the NCI preclinical antitumor drug discovery screen, in Cancer: Principles and Practice of Oncology Updates Vol. 3, no. 10* (Eds.: V. T. DeVita, Jr, S. Hellman, S. A. Rosenberg), Lippincott, Philadelphia, **1989**, pp. 1–12.
- [44] A. Eva, K. C. Robbins, P. R. Andersen, A. Srinivasan, S. R. Tronick, E. P. Reddy, N. W. Ellmore, A. T. Galen, J. A. Lautenberger, T. S. Papas, E. H. Westin, F. Wongstaal, R. C. Gallo, S. A. Aaronson, *Nature* **1982**, *295*, 116–119.
- [45] J. Sambrook, E. F. Fritsch, T. Maniatis, *Molecular cloning: a laboratory manual*, 2nd ed., Cold Spring Harbor laboratory press, Cold Spring harbor, NY, **1989**.

Received: March 26, 2008

Revised: April 29, 2008

Published online on June 9, 2008